Chapter 1

Shell Model: Woods–Saxon Potential and Ground-State J^π

"For realistic calculations, more accurate potentials are preferred... Among the various models, the Woods–Saxon potential is particularly effective."

lecture notes, PH5001

Lecture 12 showed that magic numbers beyond 20 require spin–orbit coupling, and that the choice of infinite well versus harmonic oscillator does not change those magic numbers once $\boldsymbol{\ell} \cdot \boldsymbol{s}$ is strong enough. Realistic calculations still need a finite, diffuse mean field: the **Woods–Saxon** potential. With that spectrum one reads ground-state spin and parity from the extreme single-particle filling rules [6, 1, 10].

1.1 Why infinite potentials fail as absolute models

An infinite wall forbids nucleon removal: separation energies would be infinite. Real nuclei have finite S_n and S_p. A finite square well allows separation but retains a discontinuous edge. Nuclear density and the mean field fall smoothly over a surface thickness of order 2–3 fm (Lecture 2). The potential should follow that density.

1.2 Woods–Saxon single-particle potential

The standard central mean field is

$$V_{\mathrm{WS}}(r) = -\frac{V_0}{1 + \exp\big[(r - R)/a\big]}, \tag{1.1}$$

with $R = r_0 A^{1/3}$, $r_0 \approx 1.25\,\mathrm{fm}$, diffuseness $a \approx 0.5$–$0.7\,\mathrm{fm}$, and depth $V_0 \sim 50\,\mathrm{MeV}$ chosen to match separation energies [10, 6, 1]. The potential is nearly flat and attractive in the nuclear interior, then rises smoothly through the surface to zero outside. At $r = R$ one has $V = -V_0/2$. The 10%–90% surface thickness follows directly from the Woods–Saxon shape. Define

$$f(r) = \frac{-V_{\mathrm{WS}}(r)}{V_0} = \frac{1}{1 + \exp[(r - R)/a]}.$$

Solving $f(r) = p$ gives

$$\frac{1}{p} - 1 = e^{(r-R)/a}, \qquad r(p) = R + a\ln\left(\frac{1-p}{p}\right). \tag{1.2}$$

Thus the inner 90% point and outer 10% point are

$$r(0.9) = R - a\ln 9, \qquad r(0.1) = R + a\ln 9. \tag{1.3}$$

Their radial separation is

$$t = r(0.1) - r(0.9) = 2a\ln 9 = 4a\ln 3 \approx 4.4\,a, \tag{1.4}$$

of order 2–3 fm for realistic a.

The radial Schrödinger equation for the reduced wave function $u(r)$ is

$$-\frac{\hbar^2}{2m}\frac{\mathrm{d}^2u}{\mathrm{d}r^2} + \left[V_{\mathrm{WS}}(r) + \frac{\ell(\ell+1)\hbar^2}{2mr^2}\right]u = E\,u, \tag{1.5}$$

with $u(0) = 0$. Outside the nucleus, $V \to 0$ for a neutron. It is useful to combine the potential and centrifugal terms into

$$V_{\text{eff}}(r) = V_{\mathrm{WS}}(r) + \frac{\ell(\ell+1)\hbar^2}{2mr^2}. \tag{1.6}$$

For $\ell > 0$, the positive centrifugal barrier suppresses the wave function near the origin and shifts probability toward the nuclear surface. Far outside, both terms approach zero. The radial equation then reduces to

$$\frac{\mathrm{d}^2u}{\mathrm{d}r^2} = \frac{2m|E|}{\hbar^2}\,u = \kappa^2 u \qquad (E < 0), \tag{1.7}$$

whose two solutions are $e^{+\kappa r}$ and $e^{-\kappa r}$. Normalisability eliminates the growing solution, leaving

$$u(r) \underset{r\to\infty}{\longrightarrow} C\,e^{-\kappa r}, \qquad \kappa = \sqrt{\frac{2m|E|}{\hbar^2}}. \tag{1.8}$$

Matching the interior numerical solution to this exterior exponential quantises the allowed energies. There is therefore a finite number of bound orbits, and the least-bound nucleon has a realistic separation energy of a few to tens of MeV.

The decay length $1/\kappa \propto 1/\sqrt{|E|}$ is important physics: a weakly bound neutron has a long exterior tail. Near the neutron drip line this produces diffuse skins and, for low ℓ where the centrifugal barrier is small, halo structure. A bound proton also decays, but its asymptotic tail is modified by the repulsive Coulomb potential rather than being a pure exponential at finite radius.

For protons one must add the Coulomb potential of the remaining charge distribution. A simple estimate for a uniformly charged sphere of radius R is

$$V_C(r) = \begin{cases} \dfrac{(Z-1)e^2}{8\pi\epsilon_0 R}(3 - r^2/R^2), & r \le R, \\ \dfrac{(Z-1)e^2}{4\pi\epsilon_0 r}, & r > R. \end{cases} \tag{1.9}$$

Consequently the proton well is shallower and slightly wider than the neutron well at the same A, which helps explain $N > Z$ for heavy stable nuclei [6, 1].

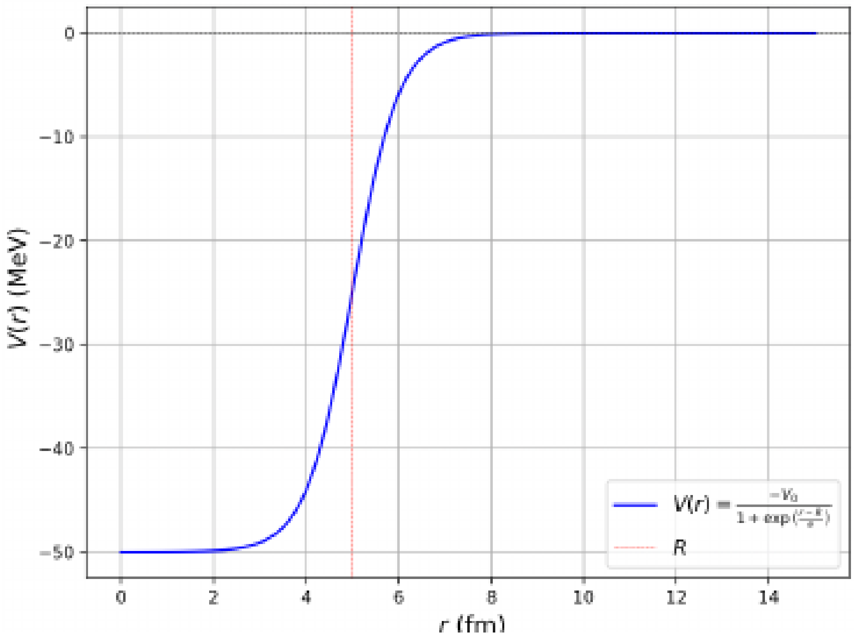

Figure 1.1: Woods–Saxon potential $V(r)$ used as the basic single-particle nuclear mean field. The red marker indicates the half-depth radius R (re-extracted with complete axes and legend from the full original PH5001 source page; Woods and Saxon [10]).

1.3 From oscillator to Woods–Saxon to spin–orbit

Compared with the oscillator, a finite diffuse well lowers high-ℓ orbitals preferentially (they live nearer the surface) and lifts accidental degeneracies such as $1d$–$2s$ and $1f$–$2p$. Typical trends when passing from oscillator (HO) to Woods–Saxon (WS) before spin–orbit:

- $1f$ drops more than $2p$;
- $1g$ drops strongly, approaching the $1f, 2p$ region;
- $1d$ and $2s$ split, with $1d$ usually lower;
- $2d$ and $3s$ descend; the uppermost level becomes $1h$.

Adding $\boldsymbol{\ell} \cdot \boldsymbol{s}$ then splits each $\ell > 0$ level: $1p \to p_{3/2}, p_{1/2}$; $1d \to d_{5/2}, d_{3/2}$; $1f \to f_{7/2}, f_{5/2}$; $1g \to g_{9/2}, g_{7/2}$; $1h \to h_{11/2}, h_{9/2}$. The magic numbers remain $2, 8, 20, 28, 50, 82, 126$, but the detailed spacings become realistic (Fig. 1.2).

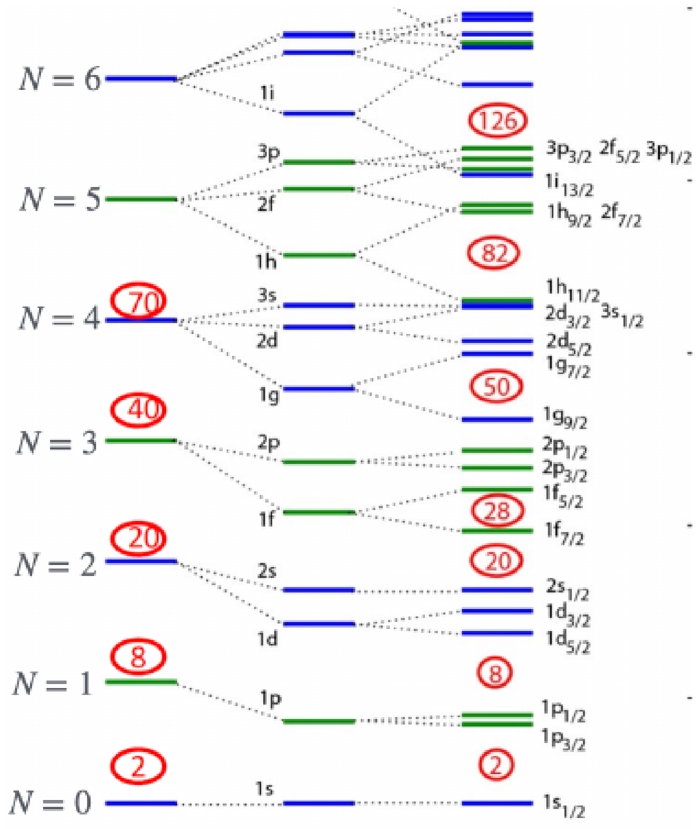

Figure 1.2: Single-particle spectrum: harmonic oscillator (HO), Woods–Saxon (WS), and Woods–Saxon plus spin–orbit (WS+LS). Red circles mark shell closures (adapted from the original PH5001 lecture figure; cf. Dunlap [1] and Krane [6]).

Key idea

Magic numbers are robust once spin–orbit is present. Energy values and intra-shell ordering depend on the central potential; Woods–Saxon is the standard realistic choice. The finite depth controls separation energies, the diffuseness controls surface physics, the centrifugal term separates different ℓ, and spin–orbit coupling separates $j = \ell \pm \frac{1}{2}$.

1.4 Extreme single-particle model

In the **extreme single-particle** (or independent-particle) limit one assumes:

1. nucleons fill the lowest available single-particle orbits;
2. residual interactions are dominated by pairing of like nucleons into $J = 0$ pairs;
3. ground-state properties of odd-A nuclei (spin, parity, magnetic moment) are carried by the last unpaired nucleon.

Even–even nuclei then have all nucleons paired. The model is most reliable near closed shells; mid-shell, configuration mixing and collective motion become essential (Lecture 15).

1.5 Spin and parity: notation

Nuclear "spin" means total angular momentum $\boldsymbol{I}$ (often written J). For a single nucleon,

$$\boldsymbol{j} = \boldsymbol{\ell} + \boldsymbol{s}, \qquad |j| = \sqrt{j(j+1)}\,\hbar, \qquad \pi = (-1)^{\ell}. \tag{1.10}$$

The spectroscopic label is I^π (or J^π). Example: a nucleon in $d_{5/2}$ ($\ell = 2$, $j = \frac{5}{2}$) has $I^\pi = \frac{5}{2}^+$.

1.6 Even–even nuclei: always 0^+

Every proton and every neutron can pair to total angular momentum zero. Consider two identical nucleons in the same $n\ell_j$ orbit. The Pauli principle restricts the allowed total angular momenta of the pair to the even values

$$I = 0, 2, \dots, 2j - 1 \tag{1.11}$$

(odd multipoles are excluded for two identical fermions in one j shell). Among these, the residual short-range attraction favours the maximum spatial overlap, which occurs for the $I = 0$ pair. That pair has positive parity regardless of whether ℓ is even or odd, because

$$\pi_{\text{pair}} = (-1)^{\ell}(-1)^{\ell} = +1. \tag{1.12}$$

With all nucleons paired,

$$I^\pi = 0^+, \tag{1.13}$$

independent of which orbits are filled. That is a robust success of the model and of experiment for essentially all even–even ground states [6, 1, 20]. The magnetic moment vanishes as well (Lecture 14).

1.7 Odd-A nuclei: last nucleon rules

Either Z or N is odd. All but one nucleon form $J = 0$ pairs; the unpaired nucleon occupies the last partially filled orbit $n\ell_j$ and determines

$$I = j, \qquad \pi = (-1)^\ell. \tag{1.14}$$

1.7.1 Example: ^{15}N

Nitrogen-15 has $Z = 7$, $N = 8$. Neutrons fill a closed shell through $1p_{1/2}$. The proton occupation is

$$(1s_{1/2})^2(1p_{3/2})^4(1p_{1/2})^1. \tag{1.15}$$

The unpaired proton is in $1p_{1/2}$ ($\ell = 1$, $j = \frac{1}{2}$), so

$$I^\pi = \tfrac{1}{2}^-, \tag{1.16}$$

in agreement with experiment.

1.7.2 Pairing can reorder occupations: ^{61}Ni

Nickel-61 has $Z = 28$, $N = 33$. The protons fill the closed $Z = 28$ shell. Above the $N = 28$ neutron core one must place five valence neutrons in the $2p_{3/2}$, $1f_{5/2}$ and $2p_{1/2}$ sequence. Two competing occupations illustrate the role of residual pairing:

$$(2p_{3/2})^4(1f_{5/2})^1 \quad \Rightarrow \quad I^\pi = \tfrac{5}{2}^-, \tag{1.17}$$
$$(2p_{3/2})^3(1f_{5/2})^2 \quad \Rightarrow \quad I^\pi = \tfrac{3}{2}^-. \tag{1.18}$$

In the second configuration the two $1f_{5/2}$ neutrons form a $J = 0$ pair, and the unpaired neutron remains in $2p_{3/2}$. Experiment finds $I^\pi = \frac{3}{2}^-$ for the ground state of ^{61}Ni [20, 21, 6], so the paired $(1f_{5/2})^2$ occupation is preferred (Fig. 1.3).

The lesson is not a universal rule that "pairing is always stronger in high-ℓ orbits", but rather that residual pairing can reorder nearby configurations when single-particle spacings are small. The extreme model still applies once the correct odd orbit is identified [6, 1].

1.7.3 Example: ^{17}O

Oxygen-17 ($Z = 8$, $N = 9$) has closed proton shells and neutrons $(1s_{1/2})^2(1p_{3/2})^4(1p_{1/2})^2(1d_{5/2})^1$ (Fig. 1.4). The valence neutron is $1d_{5/2}$, so

$$I^\pi = \tfrac{5}{2}^+. \tag{1.19}$$

Evaluated data confirm the ground state $5/2^+$ and a first excited $1/2^+$ state at 871 keV, corresponding to promotion of the valence neutron to $2s_{1/2}$ [20, 21]. Negative-parity states involve p-shell holes. Excited states of ^{17}O are treated systematically in Lecture 15.

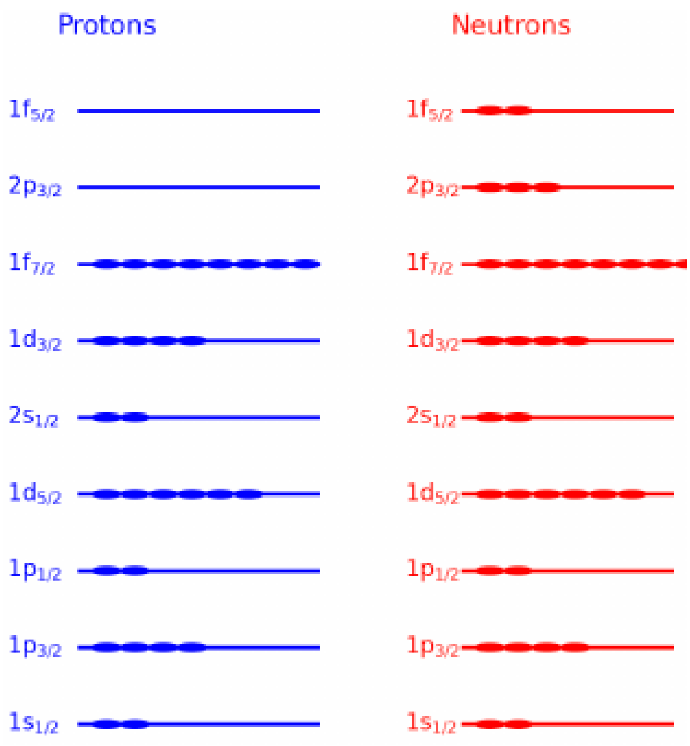

Figure 1.3: Single-particle filling for $^{61}\mathrm{Ni}_{33}$: protons (blue) and neutrons (red). The odd neutron occupies $2p_{3/2}$ rather than $1f_{5/2}$ because residual pairing of two neutrons in $1f_{5/2}$ lowers the total energy. The displayed valence occupations are $(2p_{3/2})^3(1f_{5/2})^2$ (re-extracted from the full original PH5001 source page).

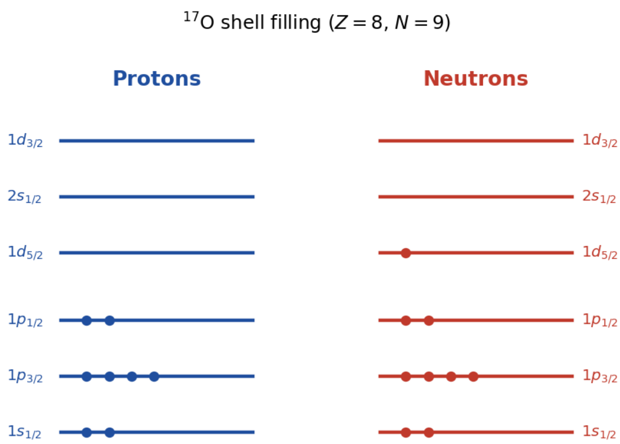

Figure 1.4: Shell-model level occupation for ^{17}O: closed proton shell and unpaired $1d_{5/2}$ neutron (adapted from the original PH5001 lecture figure).

1.8 Odd–odd nuclei

Both an unpaired proton and an unpaired neutron contribute. Their angular momenta $\boldsymbol{j}_p$ and $\boldsymbol{j}_n$ couple to a multiplet of total angular momentum

$$|j_p - j_n| \leq I \leq j_p + j_n, \tag{1.20}$$

in integer steps, with parity

$$\pi = (-1)^{\ell_p + \ell_n}. \tag{1.21}$$

The triangle rule alone does *not* select the ground-state member of the multiplet: residual proton–neutron interactions decide the ordering. Nordheim's empirical rules provide a first guide [19, 6], but they are not rigorous theorems. Few odd–odd nuclei are stable (Lecture 5); ^{14}N ($I^\pi = 1^+$) is a classic light example [20].

Key idea

Even–even: 0^+. Odd A: I^π of the last unpaired nucleon (subject to pairing reordering near closely spaced levels). Odd–odd: an allowed multiplet $|j_p - j_n| \leq I \leq j_p + j_n$, with the ground member fixed by residual pn interactions.

1.9 Pairing and the SEMF

Two nucleons in the same j orbit prefer $I_{\text{pair}} = 0$. That pairing energy is the microscopic origin of the SEMF pairing term δ (Lecture 4) and of the even–even preference for stability. Breaking a pair costs $\sim$ 1–2 MeV and is the first step toward many low-lying even–even excitations (two-quasiparticle states), while odd-A spectra often show the pure single-particle sequence until core excitations set in [6].

1.10 Further physics: proton versus neutron potentials

Because protons feel Coulomb repulsion in addition to the nuclear mean field, the proton single-particle spectrum is not identical to the neutron spectrum at the same A. Relative to neutrons, proton orbits are pushed upward, and the least-bound proton typically has a smaller separation energy near the proton drip line than the analogous neutron near the neutron drip line [6, 1].

In transfer and knockout reactions one therefore maps proton and neutron spectroscopic factors separately. Near closed shells the extreme single-particle assignments for I^π remain robust; far from stability the same residual interactions that reorder ^{61}Ni can rearrange whole sequences of levels and even dissolve traditional magic numbers. Modern shell-model and density-functional calculations keep the Woods–Saxon (or Hartree–Fock) mean field as the starting point and diagonalise a residual interaction in a truncated valence space.

1.11 Problems with solutions

Problem 13.1 — Woods–Saxon radius

For ^{208}Pb with $r_0 = 1.25\,\text{fm}$, compute $R = r_0 A^{1/3}$. If $a = 0.65\,\text{fm}$, estimate the 10%–90% surface thickness $t = 4a \ln 3$.

Solution 13.1

$$A^{1/3} = 208^{1/3} \approx 5.924, \qquad R = 1.25 \times 5.924 \approx 7.40\,\text{fm}.$$

The surface thickness is

$$t = 4a \ln 3 = 4 \times 0.65 \times \ln 3 \approx 2.86\,\text{fm},$$

consistent with electron-scattering skins [1, 6, 10].

Problem 13.2 — Ground-state J^π

Predict I^π for ^{17}O and for ^{40}Ca in the extreme single-particle model.

Solution 13.2

^{17}O: unpaired neutron in $1d_{5/2}$ ($\ell = 2$, $j = \frac{5}{2}$) $\Rightarrow \frac{5}{2}^+$. ^{40}Ca: doubly magic even–even $\Rightarrow 0^+$ [6, 20].

Problem 13.3 — ^{15}N configuration

Write the proton and neutron occupations of ^{15}N and deduce I^π.

Solution 13.3

Neutrons: closed through $1p_{1/2}$ ($N = 8$). Protons: $(1s_{1/2})^2(1p_{3/2})^4(1p_{1/2})^1$. Unpaired proton in $1p_{1/2} \Rightarrow I^\pi = \frac{1}{2}^-$ [6, 20].

Problem 13.4 — Odd–odd multiplet

An unpaired $d_{5/2}$ proton and an unpaired $p_{1/2}$ neutron form an odd–odd configuration. List the allowed I^π values and state what additional physics is needed to choose the ground member.

Solution 13.4

$$|j_p - j_n| = 2, \qquad j_p + j_n = 3,$$

so $I = 2, 3$. Parity $\pi = (-1)^{2+1} = -$, hence 2^- and 3^-. Residual proton–neutron interactions (guided empirically by Nordheim rules) select which of these is the ground state [19, 6].

Bibliography

[1] R. A. Dunlap, *An Introduction to the Physics of Nuclei and Particles* (2nd ed.), IOP Publishing, Bristol (2023), DOI: 10.1088/978-0-7503-6094-4, Ch. 3 (Nuclear composition and size).

[2] W. Demtröder, *Nuclear and Particle Physics*, Undergraduate Lecture Notes in Physics, Springer, Cham (2023).

[3] S. Petrera, *Problems and Solutions in Nuclear and Particle Physics*, UNITEXT for Physics, Springer, Cham (2019).

[4] F. Terranova, *A Modern Primer in Particle and Nuclear Physics*, Oxford University Press (2021).

[5] S. D'Auria, *Introduction to Nuclear and Particle Physics*, Undergraduate Lecture Notes in Physics, Springer, Cham (2018).

[6] K. S. Krane, *Introductory Nuclear Physics*, Wiley, New York (1988).

[7] R. Hofstadter, "Electron scattering and nuclear structure," Rev. Mod. Phys. **28**, 214 (1956).

[8] H. F. Ehrenberg, R. Hofstadter, U. Meyer-Berkhout, D. G. Ravenhall, and S. E. Sobottka, "High-Energy Electron Scattering and the Charge Distribution of Carbon-12 and Oxygen-16," Phys. Rev. **113**, 666 (1959).

[9] H. Yukawa, "On the interaction of elementary particles. I," Proc. Phys.-Math. Soc. Japan **17**, 48 (1935).

[10] R. D. Woods and D. S. Saxon, "Diffuse surface optical model for nucleon-nuclei scattering," Phys. Rev. **95**, 577 (1954).

[11] H. G. J. Moseley, "The high-frequency spectra of the elements," Phil. Mag. **26**, 1024 (1913); **27**, 703 (1914).

[12] C. F. von Weizsäcker, "Zur Theorie der Kernmassen," Z. Phys. **96**, 431 (1935).

[13] P. Cappellaro, *Introduction to Applied Nuclear Physics* (MIT OpenCourseWare / LibreTexts), CC BY-NC-SA 4.0.

[14] J.-L. Basdevant, J. Rich, and M. Spiro, *Fundamentals in Nuclear Physics: From Nuclear Structure to Cosmology*, Springer, New York (2005).

[15] D. Tong, *Particle Physics*, Lecture notes (University of Cambridge / CERN school notes).

[16] M. G. Mayer, "On closed shells in nuclei. II," Phys. Rev. **75**, 1969 (1949).

[17] O. Haxel, J. H. D. Jensen, and H. E. Suess, "On the "magic numbers" in nuclear structure," Phys. Rev. **75**, 1766 (1949).

[18] T. Schmidt, "Über die magnetischen Momente der Atomkerne," Z. Phys. **106**, 358 (1937).

[19] L. W. Nordheim, "On spins, moments, and shells in nuclei," Phys. Rev. **78**, 294 (1950).

[20] Evaluated Nuclear Structure Data File (ENSDF), National Nuclear Data Center, Brookhaven National Laboratory, `https://www.nndc.bnl.gov/ensdf/`.

[21] NuDat 3, National Nuclear Data Center, Brookhaven National Laboratory, `https://www.nndc.bnl.gov/nudat3/`.

[22] N. J. Stone, "Table of nuclear magnetic dipole and electric quadrupole moments," At. Data Nucl. Data Tables **90**, 75 (2005); updated compilations at NNDC.